American Mineralogist, Volume 74, pages 141–150, 1989

Treatment of the hydroxyl in structure-energy calculations

Richard N. Abbott, Jr.
Department of Geology, Appalachian State University, Boone, North Carolina 28608, U.S.A.
Jeffrey E. Post
Department of Mineral Sciences, Smithsonian Institute, Washington, D.C. 20560, U.S.A.
Charles W. Burnham
Department of Earth and Planetary Sciences, Harvard University, Cambridge, Massachusetts 02138, U.S.A.

Abstract

Ionic modeling of phyllosilicates and other hydrous minerals requires that a short-range pair potential for hydroxyl, O^{2-}–H^{+}, be available. Because such a potential cannot be obtained directly through the modified electron gas (MEG) formalism, we have derived Born-type short-range hydroxyl parameters by strictly empirical means. These parameters enable effective O–H modeling for hydroxyls in mica layers and brucite-like sheets and may well be applicable to hydroxyls in a wider range of environments.

Where pair-specific parameters fitting the Born expression for short-range energy [$W_{R,ij} = \lambda_{ij} \exp(-r_{ij}/\rho_{ij})$] have been determined for closed-shell cation-oxygen pairs using MEG theory, ρ values generally lie between 0.23 and 0.27 Å. Using a value for ρ_{OH} of 0.25 Å, we have determined the most appropriate values for λ_{OH} for hydroxyls in three structures—chlorite, tremolite, and clintonite—whose H positions have been accurately determined using neutron-diffraction data. A value for λ_{OH} of 30000 kJ/mol closely reproduces O-H distances and orientations in trioctahedral mica layers and in tremolite. It appears to work well whenever the hydroxyl oxygen-site potential lies in the range 2.0–2.3 e/Å. A lower λ_{OH} value of 24250 kJ/mol closely reproduces the OH configuration in the brucite sheets of chlorite and is more generally suitable when the hydroxyl oxygen-site potential is 1.2–1.6 e/Å.

Calculations with these values on hydroxyl ions in other trioctahedral and dioctahedral phyllosilicates showed that where agreement with observations based on Fourier difference maps or previous Coulomb electrostatic calculations was poor, the calculations gave results more consistent with neutron-diffraction experiments. Two energy minima were found for H in pyrophyllite, corresponding to OH orientations having c^*-O–H angles of 6° (essentially the orientation in trioctahedral phyllosilicates) and 116° (an orientation previously suggested for celadonite and glauconite). In margarite, only one energy minimum exists, which corresponds to an OH orientation normal for trioctahedral phyllosilicates. In muscovite, the calculated OH orientations depend very much on the distribution of Al and Si over the tetrahedral sites, thus suggesting that infrared-absorption studies and neutron-diffraction structural determinations of muscovite give only the average of many individual OH orientations.

Introduction

Perhaps no one has framed the problem of H in phyllosilicate structures quite as succinctly as Giese (1984) who wrote, "The hydrogen experiences a myriad of electrostatic attraction and repulsion forces." In the context of his energy calculations, the forces of repulsion refer to Coulomb electrostatic repulsions. Coulomb electrostatic calculations by Giese (1984) and by Bookin and coworkers (Bookin and Drits, 1982; Bookin et al., 1982) were concerned only with the orientation of OH dipoles and not interionic O–H distances; reasonable values for the latter were assumed. An OH dipole was allowed to pivot about the oxygen atom until the lowest Coulomb electrostatic energy was found, thus yielding the lowest-energy orientation for an OH dipole of fixed O–H distance. Our simulation of phyllosilicate structures requires that we determine both O–H orientations and distances. In order to do this, we first had to evaluate empirically an appropriate short-range O–H repulsive potential in terms that could be used in conjunction with other interionic potentials obtained through modified electron gas (MEG) theory (Muhlhausen and Gordon, 1981a, 1981b).

MEG theory provides a nonempirical, purely ionic approach for performing energy calculations on complicat-

0003–004X/89/0102–0141$02.00

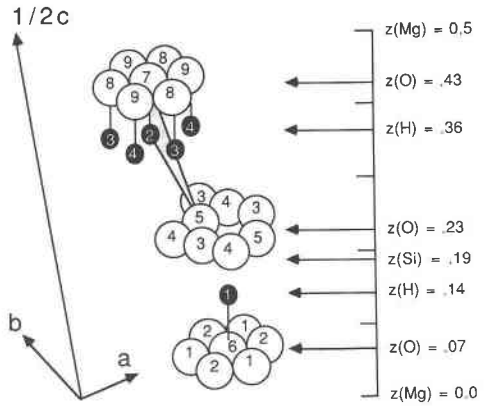

Fig. 1. The distribution of oxygen atoms (open circles labeled 1 through 9) relative to H atoms (filled circles labeled 1, 2, 3, and 4) in chlorite. The labeling of atoms is consistent with that of Joswig et al. (1980). The z coordinates for the different planes of atoms are given on the right. Atoms of the same type and having the same number are related by C-centering. In serpentine, the magnesiums at $z = 0$ and $z = 0.5$ are crystallographically equivalent, such that the c repeat is 7 Å, or one-half the 14-Å c repeat of chlorite. Hydrogen H1 of the mica layer has thirteen nearest-neighbor oxygens—including O6 of the hydroxyl pair, three each of the oxygens of types O1 and O2, and two each of types O3, O4, and O5. Hydrogen H2 of the brucite layer has six nearest-neighbor hydrogens—three each of types H3 and H4—and twelve nearest-neighbor oxygens—including O7 of the hydroxyl, three each of the oxygens of types O8 and O9 in the brucite sheet, and five oxygens of the mica layer (one of type O5 and two each of types O3 and O4). O1 and O2 are apical oxygens; O3, O4, and O5 are basal oxygens.

ed crystal structures (Post and Burnham, 1986a, 1986b, 1987). Quite simply, the procedure for determining a structure involves a search, which can be conducted in a number of ways (Busing, 1981), for the atomic arrangement having the lowest possible cohesive energy. The contribution, W_{ij}, to the total cohesive energy by the ion pair i-j can be written as the sum of two terms:

$$W_{ij} = W_{C,ij} + W_{R,ij} \quad (1)$$

where $W_{C,ij}$ is the Coulomb electrostatic energy and $W_{R,ij}$ is the short-range repulsive energy. The former is given by the expression,

$$W_{C,ij} = q_i \cdot q_j / r_{ij}, \quad (2)$$

where q_i and q_j are the formal charges on ions i and j and r_{ij} is the interionic distance. The later term, $W_{R,ij}$, arises from the overlapping of electron orbitals of neighboring ions. In their adaptation of MEG theory, Post and Burnham (1986a) used the Born formulation (Born and Huang, 1954) for the short-range repulsive energy,

$$W_{R,ij} = \lambda_{ij} \cdot \exp(-r_{ij}/\rho_{ij}), \quad (3)$$

and evaluated pair-specific parameters, λ_{ij} and ρ_{ij}, for a number of mineralogically important cations and anions.

At present, MEG theory can be applied only to closed-shell ions (Muhlhausen and Gordon, 1981a, 1981b). The method, therefore, cannot be used directly for ion pairs involving transition elements with unfilled d orbitals, or for pairs involving the hydrogen ion (H^+), which has no filled orbitals. Short-range repulsive energy terms for pairs involving H can be evaluated only for the hydride ion. There is no reason to believe, however, that repulsive energy terms appropriate for H^- can be adapted in any realistic fashion to describe the OH^- pair.

We have considered two common hydroxyl environments, both of which occur in chlorite (Fig. 1) and serpentine: OH^- in the mica layer and OH^- in the brucite sheet.

Mica-type H

The mica-type H^+ environment is illustrated by the H labeled 1 in Figure 1. The H^+ forms a short bond with one oxygen, O6, which in turn is coordinated to two or three octahedral cations (Mg, Fe, Al at $z = 0$). The O–H distance is about 0.9 Å (Bailey, 1984; Giese, 1984). The next nearest atoms to the H are twelve oxygens. Six of these (O1's and O2's) are apical oxygens, each coordinated by four cations including one tetrahedral cation (Si or Al at $z = 0.19$ in Fig. 1) and two or three octahedral cations (Mg, Fe, Al at $z = 0.0$). The remaining six are basal oxygens (O3's, O4's, and O5's), each coordinated by two tetrahedral cations (Si or Al at $z = 0.19$). The nearest-neighbor *cations* to the H^+ depend on the orientation of the OH dipole, which in turn depends on the occupancy of the tetrahedral and octahedral sites (Giese, 1984). Three OH orientations have been described (Giese, 1984), which we refer to as type-0, type-1, and type-2 throughout this paper.

Type-0 OH orientation

In the common dioctahedral micas ($^{[4]}Al/Si = 1/3$), c^*-O–H angles from 70° to 90° have been suggested on the basis of infrared-absorption studies (Serratosa and Bradley, 1958; Bassett, 1960; Vedder and McDonald, 1963), though the evidence is by no means conclusive. By comparison with the behavior of trioctahedral micas, the infrared-absorption characteristics of dioctahedral micas do not preclude a range of individual c^*-O–H angles, even to the extent that a proportion of the OH dipoles may be nearly parallel to c^*. Vedder and McDonald (1963) were very careful to point out that infrared-absorption spectra provide direct evidence regarding the orientation of the *OH transition moment,* which is only indirectly related to an *average* OH orientation. The OH transition moment may in fact reflect an average of many different, individual c^*-O–H angles. On the basis of neutron-diffraction experiments, Rothbauer (1971) determined an average c^*-O–H angle of 78° in muscovite. The mean-square displacements (msd) for H, especially the $\bar{\mu}^2(c^*,H)$ term, are extremely high in relation the msd's for other atoms in the structure (Rothbauer, 1971). The value for $\bar{\mu}^2(c^*,H)$, 0.071 Å^2, is more than 3 times greater than $\bar{\mu}^2(c^*,K)$, from 4.5 to 9 times greater than the various

$\bar{\mu}^2(c^*,O)$ terms, approximately 8 times greater than either of the $\bar{\mu}^2(c^*,{}^{[4]}Al\text{-}Si)$ terms, and 14 times greater than $\bar{\mu}^2(c^*,{}^{[6]}Al)$. The very high msd's for H reflect either a wide range of individual c^*-O–H angles or a large libration of the OH dipole.

Type-1 OH orientation

In celadonite ($^{[4]}Al/Si = 0$), c^*-O–H angles greater than 90° have been suggested (Bailey, 1984; Giese, 1984) such that two H^+ ions actually lie within the coordination polyhedron of the otherwise vacant M1 site.

Type-2 OH orientation

In trioctahedral phyllosilicates, the OH dipole is nearly parallel to c^* (essentially perpendicular to the plane defined by the O1's and O2's in Fig. 1). Analysis of infrared-absorption data lead unambiguously to this orientation (Serratosa and Bradley, 1958; Bassett, 1960; Rossman, 1984).

Brucite-type H

The brucite-type H^+ in phyllosilicate structures is illustrated by the H labeled 2 (H2) in Figure 1. This H^+ forms a short bond with one oxygen, O7, which in turn is coordinated to three octahedral cations (Mg, Fe, Al at $z = 0.5$ in Fig. 1). The next-nearest atoms to H2 include six hydrogens (H3's and H4's in Fig. 1), six oxygens (O8's and O9's) belonging to the brucite sheet, and at least five basal oxygens (O5, two O3's, two O4's) belonging to the mica sheet. The environments of hydrogens H3 and H4 in Figure 1 are similar to the environment of H2 (Joswig et al., 1980). The brucite O–H vector is nearly parallel to c^* (essentially perpendicular to the plane defined by the O7's, O8's, and O9's). Angles of the type O7–H2–O5, which is the obtuse angle between the brucite OH dipole and the vector between the H^+ and the nearest basal oxygen in the mica layer, are generally greater than 160° (Joswig et al., 1980; Bailey, 1986).

Calculations

Choice of ρ_{OH}

Post and Burnham (1986a) used MEG theory to derive values for λ_{ij} and ρ_{ij} for a variety of mineralogically important cation-oxygen pairs. The procedure employs a charged spherical shell of radius r_s, centered on the oxygen nucleus, that serves to stabilize the O^{2-} species. Following Muhlhausen and Gordon (1981a), the radius of the spherical charged shell for a particular oxygen is selected so that the shell potential at the oxygen nucleus equals the oxygen-site potential; cation-oxygen and O-O short-range interaction parameters depend on the oxygen shell radius. Values for $r_{s(O)}$ in silicate minerals typically range from about 0.9 Å to about 1.15 Å, reflecting oxygen-site potentials in the range from 0.9 to 1.1 e/Å. Examination of a variety of ρ_{ij} values (Post and Burnham, 1986a), plotted in Figure 2 as a function of $r_{s(Z)}$, where Z = O, Cl, or F, reveals a number of features: (1) In the range of common $r_{s(O)}$, ρ_{ij} values (except for $\rho_{K\text{–}O}$) all lie between 0.23 Å and 0.26 Å; (2) for cation-oxygen pairs, values of ρ_{ij} do not depend strongly on either the periodic row or group of the cation; (3) ρ_{ij} values for cation-Cl and cation-F pairs are systematically lower than the ρ_{ij} values for cation-O pairs. These observations indicate that ρ_{ij} depends essentially on the anion; changes from cation to cation are small by comparison. On the basis of these observations, we suggest that a value for $\rho_{O\text{–}H}$ of 0.25 Å is reasonably appropriate.

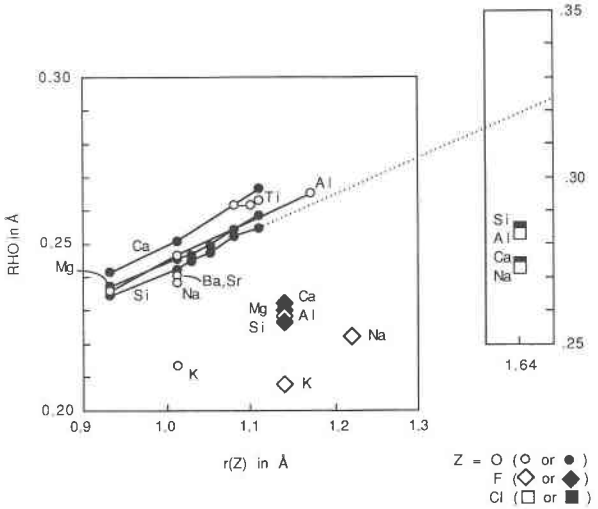

Fig. 2. Plot of ρ values for various cation-anion pairs, as a function of the shell radius of the anion, r_Z. The plot includes data from Post and Burnham (1986a) plus some new determinations by one of us (J.E.P.).

Evaluating λ_{OH}

We evaluated the short-range OH energy terms, $W_{R,OH}$ (Eq. 3), for three phyllosilicate structures in which the H positions are accurately known. The three structures include chlorite (Joswig et al., 1980), tremolite (Hawthorne and Grundy, 1976), and clintonite (Joswig et al., 1986), all of which have been refined using neutron-diffraction data. Given an acceptable ρ_{OH} value and well-known H^+ positions, our calculations permit us to obtain appropriate λ_{OH} values.

Using the table of values for λ_{ij} and ρ_{ij} in Post and Burnham (1986a), it is a simple matter to demonstrate that short-range repulsive energy terms, $W_{R,ij}$, become negligible for interionic separations greater than about 1.5 times observed nearest-neighbor distances. On the other hand, the Coulomb electrostatic terms, $W_{C,ij}$, are significant far beyond the range of nearest-neighbor distances. For these reasons, we adopted the following formulation for the site energy of H^+:

$$W(H) = W_{C,OH} + W_{R,OH} + \sum_i W_{C,(H,\ldots i)}, \qquad (4)$$

where $W_{C,OH}$ and $W_{R,OH}$ refer to the hydroxyl ion and $W_{C,(H,\ldots i)}$ refers to the Coulomb electrostatic energy of H^+

Table 1. Calculated OH distances and orientations compared with structural determinations based on neutron-diffraction data

	Observed	Calculated
Brucite OH in chlorite (after Joswig et al., 1980)		
λ (kJ/mol)	—	24250
W(H), site energy (kJ)	—	−10893
No. of neighboring oxygens	—	13
No. of neighboring hydrogens	—	6
H2–O7 (Å)	0.958	0.96
H2–O5 (Å)	1.983	1.96
O7–H2–O5 angle (°)	163.7	172.8
H2–O7–O5 angle (°)	11.0	4.8
Mica OH in chlorite (after Joswig et al., 1980)		
λ (kJ/mol)	—	30000
W(H), site energy (kJ)	—	−13075
No. of neighboring oxygens	—	13
H1–O6 (Å)	0.956	0.95
c^*-O–H angle (°)	0.0	0.3
Mica OH in clintonite (after Joswig et al., 1986)		
λ (kJ/mol)	—	30000
W(H), site energy (kJ)	—	−12414
No. of neighboring oxygens	—	13
Neighboring cations	—	Ca
O–H (Å)	0.943	0.95
c^*-O–H angle (°)	0.6	19.6
Ca–O–H angle (°)	179.9	154.3
Mica OH in tremolite (after Hawthorne and Grundy, 1976)		
λ (kJ/mol)	—	30000
W(H), site energy (kJ)	—	−13159
No. of neighboring oxygens	—	13
O–H (Å)	0.959	0.95
a^*-O–H angle (°)	0.2	3.5

Note: The labeling of atoms corresponds to labeling in Fig. 1.

paired with any ion *i*, except the hydroxyl oxygen. For practical purposes, we truncated the summation of $W_{C_i(H\ldots i)}$ terms to include only H . . . *i* distances shorter than about 4.5 Å. The summations include all the nearest oxygens in addition to the hydroxyl oxygen. For trioctahedral structures, suitable convergence did not require inclusion of nearest-neighbor cations, other than the six nearest-neighbor hydrogens in the case of the brucite environment. But for dioctahedral structures, reasonable results were achieved only when nearest-neighbor octahedral and tetrahedral cations were included.

The calculations were performed using the computer program QUICKSITE, written in Turbo Pascal for the Macintosh by one of us (R.N.A., from whom the program can be obtained). For any atom, the program determines the position of minimum site energy, given fixed positions for all neighboring atoms included in the energy calculation. Pairwise energy terms, W_{ij} (Eq. 1), can be summed over any number of nearest and nonnearest neighbors. The search for the lowest-energy configuration uses a "modified simplex method" (Cooper, 1981), which is similar to a Rosenbrock search (Busing, 1981). The simplex and Rosenbrock methods share the advantage that "saddles" in the energy map are ignored.

For each reference structure, we determined the minimum site-energy position of H^+, using up to 19 nearest-neighbor oxygens and hydrogens, depending on the local H environment. The value for λ_{OH} was adjusted manually in successive runs until the H coordinates coincided as closely as possible with observed coordinates. In subsequent tests performed on dioctahedral structures, the H^+ position was refined by using up to 30 nearest-neighbor cations and oxygens.

Results

Table 1 gives a comparison between our best calculated H^+ positions and observed H^+ positions; it also lists the λ_{OH} used for each "best" calculation. In the observed chlorite structure (Joswig et al., 1980), the three symmetrically distinct brucite-type H^+ sites have similar coordination geometries. We varied λ_{OH} for only one of these, labeled H2 by Joswig et al. (1980). The calculated O7–H2–O5 angle (see Fig. 1) is closer to 180° than the observed angle. Even so, the calculated position for H2 differs from the observed position by only 0.1 Å. Our calculated position for the one mica-type H^+, identified as H1 by Joswig et al. (1980), is essentially the same as the observed position.

Our calculated H position (Table 1) differs significantly from the observed H position for the hydroxyl in clintonite (Joswig et al., 1986). The observed position (x = 0.5966, y = 0.5, z = 0.3001) is on the mirror plane in space group $C2/m$. The very high mean-square displacement parallel to b^* for the H, $\bar{\mu}^2(b^*,H) = 0.250$ Å^2, suggests that individual hydrogens in the structure may not lie on the mirror plane and thus that individual unit cells do not have $C2/m$ symmetry. The $C2/m$ position would then represent an average of two or more H positions lying off the mirror plane. Our calculations were not constrained by $C2/m$ symmetry and yielded an off-mirror position (x = 0.5644, y = 0.4708, z = 0.3053) consistent with this interpretation. Averaging our calculated position with a mirror-related one yields coordinates rather close to those reported by Joswig et al. (1986).

For the mica-like hydroxyl in tremolite, the observed H^+ position (Hawthorne and Grundy, 1976) and our calculated position differ by only 0.06 Å.

From analysis of data in Table 1, we conclude that (1) The same λ_{OH}—30000 kJ/mol—works acceptably well for mica-type hydroxyls in three otherwise dissimilar structures; (2) the calculations reproduce O–H distances to within 1% of observed values; (3) angular relationships are difficult to reproduce exactly, but the greatest discrepancy, in clintonite, may reflect the existence of positional disorder in the reference structure; and (4) with regard to brucite-like hydroxyls in chlorite, a lower λ_{OH} value of 24250 kJ/mol reproduces the O–H distance to within 0.04%.

Calculations by one of us (C.W.B.) show that hydroxyl oxygens in different mica-type environments have comparable site potentials, within the range 2.0–2.3 e/Å. We assert that when the site potential for the hydroxyl oxygen is in this range, a value for λ_{OH} of 30000 kJ/mol should give reasonable results regardless of the structural context. On the other hand, oxygens in brucite-like environments (in lizardite or in chlorite) have significantly lower

TABLE 2. Calculated O–H distances and orientations for trioctahedral phyllosilicates, compared with determinations based on X-ray diffraction data

	Observed	Calculated	
Talc (after Rayner and Brown, 1973) without neighboring cations			
λ (kJ/mol)	—	30000	
W(H), site energy (kJ)	—	−13185	
No. of neighboring oxygens	—	13	
Neighboring cations	—	—	
x(H)	0.2246*	0.2310	
y(H)	0.1677*	0.1569	
z(H)	0.2091*	0.2135	
O–H (Å)	0.9*	0.95	
*c**-O–H angle (°)	0	6.2	
Talc (after Rayner and Brown, 1973) with neighboring cations			
λ (kJ/mol)	—	30000	
W(H), site energy (kJ)	—	540	
No. of neighboring oxygens	—	13	
Neighboring cations	—	3Mg, 6Si	
x(H)	0.2246*	0.2276	
y(H)	0.1677*	0.1670	
z(H)	0.2091*	0.2164	
O–H (Å)	0.9*	0.97	
*c**-O–H angle (°)	0	0.5	
Mica OH in chlorite (after Bailey, 1986)			
λ (kJ/mol)	—	30000	
W(H), site energy (kJ)	—	−13061	
No. of neighboring oxygens	—	13	
x(H)	0.3670	0.3781	
y(H)	0.3314	0.3326	
z(H)	0.1405	0.1396	
O–H (Å)	0.9644	0.95	
*c**-O–H angle (°)	0.58	4.8	
Brucite OH in chlorite for Bailey's (1986) H4 hydrogen			
λ (kJ/mol)	—	24250	21750
W(H), site energy (kJ)	—	−10874	−10943
No. of neighboring oxygens	—	13	13
No. of neighboring hydrogens	—	6	6
x(H)	0.6181	0.6288	0.6288
y(H)	0.1525	0.1472	0.1503
z(H)	0.3730	0.3618	0.3719
H4–O9 (Å)	0.8102	0.98	0.83
H4–O4 (Å)	2.1267	1.95	2.10
O9–H4–O4 angle (°)	164.88	171.0	170.4

TABLE 2.—*Continued*

	Observed	Calculated	
Brucite OH in chlorite for Bailey's (1986) H2 hydrogen			
λ (kJ/mol)	—	24250	21000
W(H), site energy (kJ)	—	—	−11216
No. of neighboring oxygens	—	13	13
No. of neighboring hydrogens	—	6	6
x(H)	0.0816	—	0.0449
y(H)	0.3356	—	0.3381
z(H)	0.3681	—	0.3721
H2–O7 (Å)	0.8942	—	0.90
H2–O5 (Å)	2.0192	—	2.03
O7–H2–O5 angle (°)	176.67	—	163.8
Mica OH in lizardite (after Mellini and Zanazzi, 1987)			
λ (kJ/mol)	—	30000	22400
W(H), site energy (kJ)	—	−13077	−13318
No. of neighboring oxygens	—	13	13
x(H)	0.0	−0.0001	0.0
y(H)	0.0	−0.0002	0.0
z(H)	0.2	0.1765	0.203
O–H (Å)	0.7840	0.95	0.76
*c**-O–H angle (°)	0	0	0
Brucite OH in lizardite (after Mellini and Zanazzi, 1987)			
λ (kJ/mol)	—	24250	27400
W(H), site energy (kJ)	—	−10727	−10661
No. of neighboring oxygens	—	13	13
No. of neighboring hydrogens	—	6	6
x(H)	0.58	0.6345	0.6274
y(H)	0.0	−0.0001	0.0
z(H)	0.738	0.7121	0.7305
H2–O7 (Å)	1.1675	0.90	1.04
H2–O5 (Å)	1.8857	2.14	2.01
O7–H2–O5 angle (°)	169.36	171.7	172.2

Note: The atoms are identified according to the labeling in Fig. 1.
* Taken as the initial position; no observed position available.

site potentials, from 1.2 to 1.6 e/Å; hence the most appropriate λ_{OH} value under these circumstances ought to be correspondingly lower. Such direct proportionality between anion site potential and λ is consistent with variation in other cation-anion pairs (Post and Burnham, 1986a) and is expected on theoretical grounds.

TRANSFERABILITY OF OH SHORT-RANGE POTENTIALS TO OTHER TRIOCTAHEDRAL STRUCTURES

The transferability of the proposed values for λ_{OH} and ρ_{OH} from one structure to another can be assessed by carrying out similar calculations on additional structures. In this context, we report the results of attempts to predict H positions in talc (Rayner and Brown, 1973), another chlorite (Bailey, 1986), and lizardite (Mellini and Zanazzi, 1987). These three structures were determined using X-ray diffraction data. Our initial H^+ positions for chlorite and lizardite were those reported by Bailey (1986) and Mellini and Zanazzi (1987), respectively, from Fourier difference maps; for talc, we selected an initial position yielding O–H parallel to *c** and 0.9 Å long. Results of our calculations are reported in Table 2.

Talc calculations were performed both with and without the nine nearest-neighbor cations, which include three magnesiums and six silicons. The calculated O-H distances differed by only 0.02 Å, whereas the orientation of the O-H bond differed by about 5.7°. The calculated position for the mica-type H^+ in chlorite is comparable to the position suggested by Bailey (1986).

Mellini and Zanazzi (1987) reported an unusually short O-H distance, 0.784 Å, for the mica-type OH in lizardite. Using λ_{OH} = 30000 kJ/mol, we calculate an O-H distance more in line with those observed in other structures (Table 1). The very short observed O-H distance was reproducible only by using a substantially reduced value for λ_{OH}. Given the uncertainties in interpreting small electron-density residuals in Fourier difference maps, it is not at all clear that the H position reported by Mellini and

TABLE 3. Calculated O–H distances and orientations for dioctahedral phyllosilicates

	Initial	Min 1	Min 2
Pyrophyllite (after Lee and Guggenheim, 1981)			
λ (kJ/mol)	—	30000	30000
W(H), site energy (kJ)	—	2668	2597
x(H)	0.1406	0.1224	0.2503
y(H)	0.1062	0.1036	0.1830
z(H)	0.1268	0.0579	0.2147
O–H (Å)	0.9575	1.02	0.99
*c**-O–H angle (°)	78.0	115.9	6.1
Margarite (after Guggenheim and Bailey, 1975)			
λ (kJ/mol)	—	—	30000
W(H), site energy (kJ)	—	—	2504
x(H)	0.8970	—	0.9362
y(H)	0.1370	—	0.0511
z(H)	0.0830	—	0.0988
O–H (Å)	0.9414	—	0.98
*c**-O–H angle (°)	46.18	—	13.0
Muscovite (after Richardson and Richardson, 1982)			
λ (kJ/mol)	—	30000	30000
W(H), site energy (kJ)	—	2406	2367
x(H)	—	0.8582	0.9675
y(H)	—	0.1478	0.0673
z(H)	—	0.0286	0.0988
O–H (Å)	—	1.01	0.96
*c**-O–H angle (°)	—	116.1	3.9

Note: In muscovite the charge was set at +3.75 on each of the six nearest-neighbor tetrahedral cations.

Zanazzi (1987) is correct. It is noteworthy that a λ_{OH} of 30000 kJ/mol consistently produced expectable O-H distances, even in lizardite.

Bailey (1986) provided atomic coordinates for three symmetrically distinct brucite-type hydrogens in chlorite. We report in Table 2 our determination of atomic coordinates for the hydrogens associated with the shortest and longest O-H distances. For the hydroxyl with the shortest O-H distance, using λ_{OH} = 24250 kJ/mol gave a distance consistent with the distances reported in Table 1. Again, as with lizardite, the very short observed O-H distance was approachable only when we used an even lower value for λ_{OH}. In the second case, for the longest observed O-H distance, when we used λ_{OH} = 24250 kJ/mol, no minimum could be located at all. The H, under the influence of the other oxygens, drifted to an unreasonable distance away from the hydroxyl oxygen. The observed structure could be reproduced, however, by reducing λ_{OH} to 21000 kJ/mol. The behavior of the H atom in these two cases suggests that a somewhat reduced λ_{OH}, as low as 21000 or 22000 kJ/mol, may be appropriate for some brucite-type OH pairs in chlorite. As was mentioned earlier, these low values for λ_{OH} reflect the unusually low site potentials for oxygens in brucite-type hydroxyl environments (1.2–1.6 e/Å).

TRANSFERABILITY OF OH SHORT-RANGE POTENTIALS TO DIOCTAHEDRAL STRUCTURES

Calculations were performed on three additional dioctahedral phyllosilicates: pyrophyllite (Lee and Guggenheim, 1981), margarite (Guggenheim and Bailey, 1975, 1978), and muscovite (Richardson and Richardson, 1982). Coordinates for H in margarite were predicted by Giese (in Guggenheim and Bailey, 1975) on the basis of Coulomb electrostatic calculations; these are the initial H coordinates reported for margarite in Table 3 (c^*-O–H = 46.2°). Later, Giese (1979) offered a revised orientation for hydroxyl in the same margarite (c^*-O–H = 84.2°). In separate Coulomb electrostatic calculations, referred to the same margarite, Bookin and Drits (1982) offered a third orientation with c^*-O–H = 70.0°.

Except for Al-Si ordering in margarite (Guggenheim and Bailey, 1975), the unit layer in each of these structures has approximately $C2/m$ symmetry. The OH dipole lies approximately in the pseudo–mirror plane, which is close to (110) in muscovite and margarite and to ($\bar{1}$10) in pyrophyllite. In most of the calculations, the OH dipoles remained relatively close to the pseudo–mirror plane.

Our calculations (Table 3) were carried out with 16 nearest-neighbor oxygens, the six nearest octahedral aluminums, the six nearest tetrahedral cations, the nearest other H, and, in the cases of margarite and muscovite, the nearest interlayer cation (Ca^{2+} or K^+). Among the 16 nearest-neighbor oxygens were included all six oxygens forming the coordination polyhedron of the vacant M1 site. The H whose position we refined was related to the nearest other H by inversion through the vacant M1 site. In marked contrast to the trioctahedral phyllosilicate calculations, reasonable OH orientations and O–H distances could not be determined unless the tetrahedral and octahedral cations were included. This difference in behavior simply reflects the fact that in trioctahedral phyllosilicates, the symmetry of the cation distribution is similar to that of the anions; thus they both influence the orientation of the OH dipole in more or less the same way. In dioctahedral phyllosilicates, however, one-third of the octahedral sites are vacant, and the influence of the cations on the orientation of the OH dipole is very different from that of the anions.

Pyrophyllite

For pyrophyllite, the initial c^*-O–H angle (78°) was set close to an anticipated result (Giese, 1984). The initial position is not critical, however, so long as it is not too far removed from a possible position. Calculations using λ_{OH} of 30000 kJ/mol indicated two minimum-energy OH orientations (Min 1 and Min 2 in Table 3), neither of which corresponded to the anticipated type-0 OH orientation. One local minimum, Min 2 (Table 3), is consistent with OH orientations in trioctahedral phyllosilicates (type-2), whereas the other local minimum, Min 1, is consistent with the OH orientation in celadonitic micas and glauconite (type-1). Figure 3 is a contour map of site energies for H in the unit-layer pseudo–mirror plane, (110). Note that the two minima are at opposite ends of a long narrow energy trough, the axis of which is relatively flat. The initial, anticipated H position, consistent with determinations based on Coulomb electrostatic energies alone (Giese, 1984), lies essentially on the axis of the low-energy trough but between the two minima,

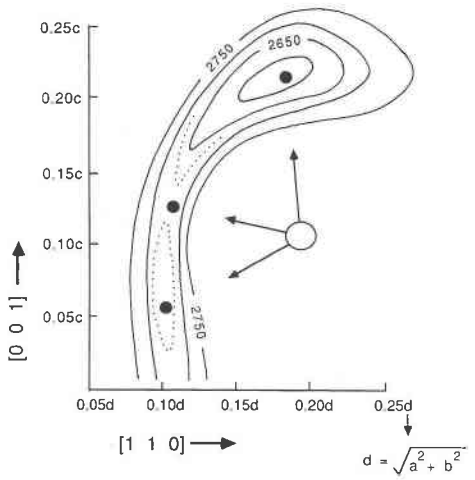

Fig. 3. Map of calculated site energies (λ_{OH} = 30000 kJ/mol) for different H positions in the (110) plane of pyrophyllite. Contour interval for the solid contours is 50 kJ; dotted contour is for 2680 kJ. Large open circle is the oxygen of the hydroxyl; three small, filled circles show the initial H position and the calculated H positions for the minima reported in Table 3.

hence at a higher energy. Local minimum Min 2 has a lower energy relative to Min 1; hence it is the *primary minimum*; minimum Min 1 is a *secondary minimum.*

Margarite

In spite of our best efforts to perturb the initial H position or adjust λ_{OH}, the calculated H position in margarite persisted in coinciding with an energy minimum of type-2 (Min 2, Table 3), in the trioctahedral configuration. This result contradicts conflicting H positions based on Coulomb electrostatic interactions alone (Guggenheim and Bailey, 1975; Giese, 1979; Bookin and Drits, 1982), and highlights well the errors than can result from neglecting short-range OH repulsive energy terms in calculations of structure configuration.

Muscovite

Although well documented as an incorrect procedure (e.g., Post and Burnham, 1987), we initially assigned each tetrahedral cation in muscovite a hybrid charge of 3.75, consistent with an Al/Si ratio of ⅓. Only energy minima of types 1 and 2 were located (Table 3). An energy minimum of type-0 could not be found by varying λ_{OH}. Subsequently, calculations were performed for 18 different arrangements of Al and Si over the six tetrahedral sites (Fig. 4a) closest to the H. The eighteen arrangements (described in Table 4 in conjunction with Fig. 4a) included all possible Al-Si orderings consistent with the aluminum avoidance principle (Loewenstein, 1954; Herrero et al., 1985; Sanz et al., 1986). All calculations used λ_{OH} = 30000 kJ/mol. For each Al-Si ordering, calculations were performed using two starting positions for H, close to positions analogous to the type-1 and type-2 minima in pyrophyllite. Results of these calculations are presented in Figure 4 and Table 4.

Analysis of Figure 4 and Table 4 yields several important features: (1) The minimum-energy position for H depends very much on the distribution of Al and Si over the tetrahedral sites closest to the H. Primary and secondary energy minima are possible and are consistent with either of two general OH orientations like the two OH orientations identified for pyrophyllite (Fig. 3). (2) There are thirteen Al-Si orderings that have both a primary and a secondary minimum. There are five Al-Si orderings that have only one minimum. (3) With one exception, when there are two minima for a given Al-Si ordering, the type-2 minimum (c*-O–H < 30°) is primary, and the type-1 minimum (c*-O–H > 90°) is secondary. This includes all of the orderings of 2Al + 4Si and four of the six orderings of 1Al + 5Si. In the exceptional case, the minimum having the lower energy is represented by a small filled circle, and the minimum having the higher energy is represented by a small open circle. The large, open circle is the oxygen of the OH pair. Two clusters of positions are identified as Min 1 and Min 2, which correspond respectively to two types of energy minima. (c) Projection down the c axis of the calculated positions for H (small, filled circles).

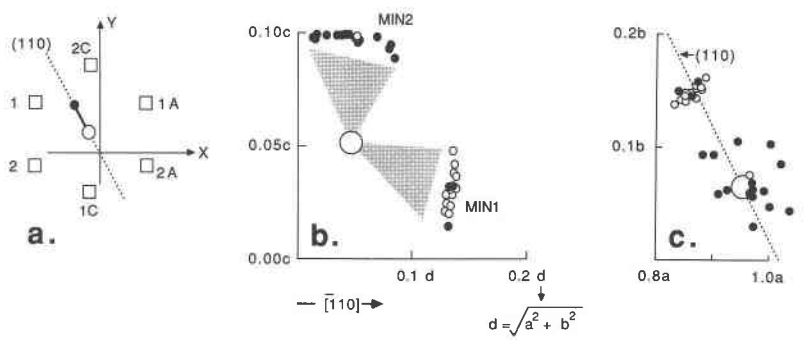

Fig. 4. (a) Projection onto (001) of the six tetrahedral sites (open squares) closest to the H (small, filled circle) in muscovite. The OH pair (the open circle is the oxygen) lies in (110), the trace of which is shown as a dotted line. Labeling of the tetrahedral sites refers to Table 4. (b) Projection onto (110) of calculated minimum-energy positions for H (small, filled and open circles). Many of the Al-Si orderings described in Table 4 have two minimum-energy positions for H (Table 4). For each such

TABLE 4. Calculated O–H distances and c^*-O–H angles for different arrangements of Al and Si on tetrahedral sites in muscovite

Case	Tetrahedral sites						O–H (Å)	c^*-O–H (°)	Type of minimum	W(H) (kJ)
	1	1A	1C	2	2A	2C				
					3Al + 3Si					
1	Al	Al	Al	Si	Si	Si	0.97	1.4	2	1692
2	Si	Si	Si	Al	Al	Al	0.98	3.5	2	1692
					2Al + 4Si					
3	Al	Al	Si	Si	Si	Si	0.96	24.9	2	2149
							1.00	106.3	1	2234
4	Al	Si	Al	Si	Si	Si	0.99	12.8	2	2129
5	Si	Al	Al	Si	Si	Si	0.98	11.7	2	2091
							1.01	121.6	1	2316
6	Si	Si	Si	Al	Al	Si	0.98	11.3	2	2105
							0.99	116.7	1	2263
7	Si	Si	Si	Al	Si	Al	0.96	27.5	2	2140
							0.96	93.46	1	2164
8	Si	Si	Si	Si	Al	Al	1.02	22.6	2	2147
							0.97	101.2	1	2203
9	Al	Si	Si	Si	Al	Si	0.97	3.9	2	2150
							1.00	112.4	1	2280
10	Si	Al	Si	Al	Si	Si	0.95	3.8	2	2148
							0.98	112.6	1	2224
11	Si	Si	Al	Si	Si	Al	0.97	4.3	2	2133
							0.98	105.4	1	2207
					1Al + 5Si					
12	Al	Si	Si	Si	Si	Si	1.02	112.0	1	2549
13	Si	Al	Si	Si	Si	Si	0.97	17.9	2	2568
							1.04	121.2	1	2590
14	Si	Si	Al	Si	Si	Si	0.99	19.5	2	2529
							1.05	125.2	1	2628
15	Si	Si	Si	Al	Si	Si	0.97	21.4	2	2569
							1.02	114.3	1	2595
16	Si	Si	Si	Si	Al	Si	0.99	21.6	2	2533
							1.05	125.7	1	2631
17	Si	Si	Si	Si	Si	Al	1.02	112.4	1	2543
					6Si					
18	Si	Si	Si	Si	Si	Si	1.12	130.0	1	2959
							0.95	6.2	2	3041

Note: The labeling of sites is explained in Fig. 4a. For each of the cases 1, 2, 4, 12, and 17, there is only one energy minimum.

tional 6Si case (18 in Table 4), the low energy of the type-1 OH orientation must be due in large part to repulsion by the interlayer K^+ cation, because a high sum of tetrahedral cation charges alone does not, by analogy with pyrophyllite, favor the type-1 OH orientation. (4) In the five cases where only one energy minimum was identified, the H^+ proceeded to the same minimum position regardless of its starting position. Both Al-Si orderings of 3Al + 3Si yielded type-2 minima (the trioctahedral configuration). Not surprisingly, when the sum of the cation charges is low, a type-2 minimum is permitted by virtue of reduced repulsion between the tetrahedral cations and the H. By analogy, it is tempting to explain the primary type-1 minima of the ordering cases 12 and 17 (Table 4) as the result of increased repulsion due to the high sum of tetrahedral cation charges in these 1Al + 5Si arrangements. But here the relationship is not so clear because four of the 1Al + 5Si orderings have primary type-2 minima. (5) In Figures 4b and 4c, each of the small, filled circles gives the H position for a primary minimum. Only three of the primary minima are consistent with a type-1 OH orientation. Only one secondary minimum (small, open circles) is consistent with the type-2 OH orientation. The distribution of primary and secondary minima in Figures 4b and 4c suggests that the type-2 OH orientation (c^*-O–H < 30°) should be more important than the type-1 OH orientation whenever there is Al in one or more tetrahedral sites.

The common 1:3 ratio of tetrahedral Al to Si cannot be satisfied by any of the four compositions described in Table 4. If the compositionally extreme situations—6Si and 3Al + 3Si—are discounted as statistically unimportant, then a structure having the common Al/Si ratio would consist of equal numbers of two compositionally distinct kinds of six-membered tetrahedral rings, 2Al + 4Si and 1Al + 5Si. All of the former yielded primary minima of type-2. At least half of the six-membered rings in an extended sheet of tetrahedra would have associated hydrogens in positions consistent with minima of this type. The remaining hydrogens, in 1Al + 5Si tetrahedral rings, could be at primary minima of either type-2 or type-1. However, if the different 1Al + 5Si orderings are

equally likely, then most of the associated hydrogens would be at minima of type-2. Presumably the $C2/c$-averaged position for H in muscovite would be somewhere in the range of the type-2 OH orientations (c^*-O–H < 30°). This contradicts predictions based on calculations using Coulomb electrostatic terms alone (Giese, 1979, 1984; Bookin and Drits, 1982; Bookin et al., 1982) in which the O-H distances were not varied. It is important to observe, in Figure 3, that a circle, centered on the oxygen and having a radius defined by the distance to the false type-0 minimum, intersects neither the type-1 minimum nor the type-2 minimum. But the lowest energy on the circle, though not particularly well defined, appears to be closer to the false minimum. Thus a mapping of Coulomb electrostatic energy alone in the vicinity of the hydroxyl would be unlikely to reveal the two energy minima.

Conclusions

1. Values for ρ_{ij} for cation-anion pairs depend most strongly on the anion. For ion pairs involving oxygen, ρ values are between 0.23 Å and 0.27 Å over a wide range of shell radii for oxygen. We believe a value of 0.25 Å for ρ_{OH} is reasonable.

2. Using ρ_{OH} = 0.25 Å, λ_{OH} is about 30000 kJ/mol for hydroxyls in the mica-type environment. These values for ρ_{OH} and λ_{OH} work well when the site potential for the hydroxyl oxygen is close to 2 e/Å, which is the situation for mica-type hydroxyls in a wide range of structures, including chlorite, lizardite, tremolite, talc, clintonite, pyrophyllite, margarite, and muscovite. Neither the occupancy of the octahedral site (dioctahedral versus trioctahedral) nor the nature of the interlayer region (brucite sheet versus A sites with vacancies or K^+ or Ca^{2+} ions) seems to have much influence on the most appropriate value of λ_{OH} for hydroxyls in mica-type environments.

3. Using ρ_{OH} of 0.25 Å, λ_{OH} is about 24250 kJ/mol for hydroxyls in the brucite-type environment. These values may be appropriate when the site potential for the hydroxyl oxygen is in the range of 1.2–1.6 e/Å. The most appropriate value for λ_{OH} is subject to greater variation in brucite-type hydroxyls than in mica-type hydroxyls.

4. Two OH orientations are possible in dioctahedral phyllosilicates. The different orientations are distinguished by different c^*-O–H angles: greater than 90°, as in celadonitic or glauconitic micas, or close to zero, as in trioctahedral phyllosilicates. The two orientations correspond to two possible energy minima. Both kinds of energy minima were identified in pyrophyllite; the primary minimum has a c^*-O–H angle of approximately 6°. Only one energy minimum, having the trioctahedral OH configuration, was identified in margarite (c^*-O–H = 13°).

5. The orientation of the OH dipole in muscovite depends on the distribution of Al and Si on the six nearest tetrahedral sites. Only two general OH orientations seem to be important: c^*-O–H < 30° and c^*-O–H > 90°. In most cases having Al in one or more tetrahedral sites, the primary energy minimum has the orientation with c^*-O–H < 30°. With no tetrahedral Al, as in celadonite, the primary energy minimum coincides with the latter orientation having c^*-O–H > 90°. By all indications, most of the OH dipoles in muscovite should be oriented such that the c^*-O–H angle is less than 30°. The presence of secondary energy minima separated by low-energy barriers from nearby primary minima suggests that under suitable excitation conditions, the OH dipole may very well exist in orientations with c^*-O–H > 90°. It may be that lattice strains due to local ordering of tetrahedral Al and Si create just such circumstances. If so, then in the $C2/c$-averaged structure for muscovite, the OH orientation may be controlled by the proportions of many different, individual OH orientations like those represented by the primary and secondary minima in Figure 4 and Table 4. An *average* OH orientation with the c^*-O–H angle between 70° and 90° (Giese, 1979, 1984; Bookin and Drits, 1982; Bookin et al., 1982) may be reasonable.

Acknowledgments

The research was supported by NSF Grant EAR 87-20666 to C.W.B. We greatly appreciate the helpful comments and suggestions offered by S. W. Bailey, Y. Ohashi, and D. Bish.

References cited

Bailey, S.W. (1984) Crystal chemistry of the micas. Mineralogical Society of America Reviews in Mineralogy, 13, 13–60.

——— (1986) Re-evaluation of ordering and local charge balance in 1a chlorite. Canadian Mineralogist, 24, 649–654.

Bassett, W.A. (1960) Role of hydroxyl orientation in mica alteration. Geological Society of America Bulletin, 71, 449–456.

Bookin, A.S., and Drits, V.A. (1982) Factors affecting orientation of OH-vectors in micas. Clays and Clay Minerals, 30, 415–421.

Bookin, A.S., Drits, V.A., Rozhdestvenskaya, I.V., Semenova, T.F., and Tsipursky, S.I. (1982) Comparison of OH-bonds in layer silicates by diffraction methods and electrostatic calculations. Clays and Clay Minerals, 30, 409–414.

Born, M., and Huang, K. (1954) Dynamical theory of crystal lattices, p. 19–37. Oxford University Press, London.

Busing, W.R. (1981) WMIN, a computer program to model molecules and crystals in terms of potential energy functions. U.S. National Technical Information Service, ORNL-5747.

Cooper, J.E. (1981) Introduction to Pascal for scientists, 260 p. Wiley, New York.

Giese, R.F., Jr. (1979) Hydroxyl orientations in 2:1 phyllosilicates. Clays and Clay Minerals, 27, 213–223.

——— (1984) Electrostastic energy models of micas. Mineralogical Society of America Reviews in Mineralogy, 13, 105–144.

Guggenheim, S., and Bailey, S.W. (1975) Refinement of the margarite structure in subgroup symmetry. American Mineralogist, 60, 1023–1029.

——— (1978) Refinement of the margarite structure in subgroup symmetry: Correction, further refinement, and comments. American Mineralogist, 63, 186–187.

Hawthorne, F.C., and Grundy, H.D. (1976) The crystal chemistry of the amphiboles. IV. X-ray and neutron diffraction refinements of the crystal structure of tremolite. Canadian Mineralogist, 14, 334–345.

Herrero, C.P., Sanz, J., and Serratosa, J.M. (1985) Tetrahedral cation ordering in layer silicates by ^{29}Si NMR spectroscopy. Solid State Communications, 53, 151–154.

Joswig, W., Fuess, H., Rothbauer, R., Takéuchi, Y., and Mason, S.A. (1980) A neutron diffraction study of a one-layer triclinic chlorite (penninite). American Mineralogist, 65, 349–352.

Joswig, W., Anthauer, G., and Takéuchi, Y. (1986) Neutron-diffraction and Mössbauer spectroscopic study of clintonite (xanthophyllite). American Mineralogist, 71, 1194–1197.

Lee, J.H., and Guggenheim, S. (1981) Single crystal X-ray refinement of pyrophyllite-*1Tc*. American Mineralogist, 66, 350–357.

Loewenstein, W. (1954) The distribution of aluminum in the tetrahedra of silicates and aluminates. American Mineralogist, 58, 92–96.

Mellini, M., and Zanazzi, P.F. (1987) Crystal structures of lizardite-*1T* and lizardite-*2H1* from Coli, Italy. American Mineralogist, 72, 943–948.

Muhlhausen, C., and Gordon, R.G. (1981a) Electron-gas theory of ionic crystals, including many-body effects. Physical Review, B23, 900–923.

——— (1981b) Density-functional theory for the energy of crystals: Test of the ionic model. Physical Review, B24, 2147–2160.

Post, J.E., and Burnham, C.W. (1986a) Ionic modeling of mineral structures and energies in the electron gas approximation: TiO_2 polymorphs, quartz, forsterite, diopside. American Mineralogist, 71, 142–150.

——— (1986b) Modeling tunnel-cation displacements in hollandites using structure-energy calculations. American Mineralogist, 71, 1178–1185.

——— (1987) Structure-energy calculations on low and high albite. American Mineralogist, 72, 507–514.

Rayner, J.H., and Brown, G. (1973) The crystal structure of talc. Clays and Clay Minerals, 21, 103–114.

Richardson, S.W., and Richardson, J.W., Jr. (1982) Crystal structure of pink muscovite from Archer's Post, Kenya: Implications for reverse pleochroism in dioctahedral micas. American Mineralogist, 67, 69–75.

Rossman, G.R. (1984) Spectroscopy of micas. Mineralogical Society of America Reviews in Mineralogy, 13, 145–181.

Rothbauer, R. (1971) Untersuchung eines *2M1*-muskovits mit neutronenstrahlen. Neues Jahrbuch für Mineralogie Monatshefte, 143–153.

Sanz, J., Herrero, C.P., and Serratosa, J.M. (1986) Tetrahedral cation distribution in phyllosilicates 2:1 by ^{29}Si NMR spectroscopy. International Mineralogical Association Abstracts with Program, 14, 220.

Serratosa, J.M., and Bradley, W.F. (1958) Determination of the orientation of OH bond axes in layer silicates by infrared absorption. Journal of Physical Chemistry, 62, 1164–1167.

Vedder, W., and McDonald, R.S. (1963) Vibrations of the OH ions in muscovite. Journal of Chemical Physics, 38, 1583–1590.

Manuscript received February 12, 1988
Manuscript accepted October 5, 1988